FULL PAPER

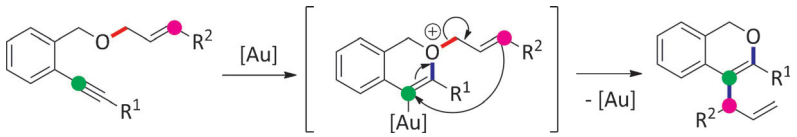

The Golden Key: Allylic inversion and crossover experiments reveal a sigmatropic rearrangement as a key step in the gold-catalyzed intramolecular allyl transfer in *ortho*-alkinyl benzyl allyl ethers.

Sigmatropic Rearrangement

*Martin Ackermann, Janina Bucher, Melissa Rappold, Katharina Graf, Frank Rominger, A. Stephen K. Hashmi** ____ ▮▮▮▮–▮▮▮▮

[3,3]-Sigmatropic Rearrangement Step in the Gold-Catalyzed Cyclization of Allyl-(*ortho*-alkinylphenyl)methyl Ethers

DOI: 10.1002/asia.201300324

[3,3]-Sigmatropic Rearrangement Step in the Gold-Catalyzed Cyclization of Allyl-(*ortho*-alkinylphenyl)methyl Ethers

Martin Ackermann, Janina Bucher, Melissa Rappold, Katharina Graf, Frank Rominger, and A. Stephen K. Hashmi*[a]

Abstract: The gold-catalyzed conversion of allyl-(*ortho*-alkynylphenyl)-methyl ethers was investigated, and allylated isochromenes were obtained. An optimization of the catalysis conditions with respect to different phosphane and carbene ligands on gold, different counterions, and different solvents was conducted. Subsequently, the scope and limitations of this reaction were investigated with 21 substrates. The mechanistic studies show an allylic inversion, as supported by NMR data and an X-ray crystal structure analysis, as well as an intermolecular reaction, as determined by crossover experiments. There is no competition of protodeauration even in the presence of water. All these observations differ from other related conversions and clearly indicate product formation by a [3,3]sigmatropic rearrangement in the step forming the new C–C bond.

Keywords: alkenes · alkynes · ethers · gold · heterocycles

Introduction

In 1988, Tsuda and Saegusa published the first example of a transition-metal-catalyzed heterocyclization with an allylic migration in a domino reaction.[1] Starting with allylic esters of homopropargylic acid **1**, they accomplished the lactonization of the ester, the fragmentation of the allylic moiety, and the subsequent C–C-bond formation that yielded the rearranged products **4** (Scheme 1).

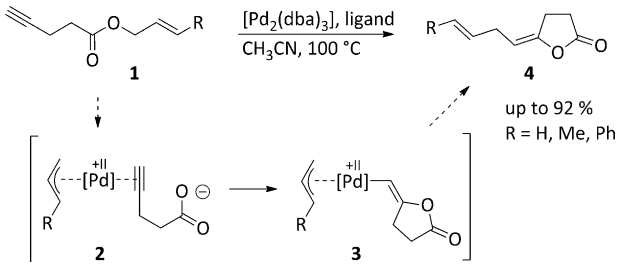

Scheme 1. Lactonization combined with an allylic shift according to Tsuda and Saegusa.[1]

During the last 20 years, related transition-metal-catalyzed cyclization–rearrangement sequences have been reported, and an array of different heterocyclic motifs have been built up using this strategy.[2] Amongst these, palladium-[2a–f] and platinum-catalyzed[2g–o] reactions played a dominating role for years until Nakamura et al. established a gold-catalyzed synthesis of benzothiophene using the same methodology.[2p] Since the field of homogeneous gold catalysis was (and still is) growing exponentially,[3] it is not surprising that the number of examples in which gold catalysts were used in a cyclization–rearrangement methodology for forming highly substituted heterocycles has risen tremendously.[2p–ae] Among these examples, benzannulation reactions play an important role; from easily available starting materials, product scaffolds of high importance like indoles,[2b,f,i,m,n,q,ag] benzofurans,[2c,d,e,j,k,l] or isocoumarines[2k,y,z,af] could be synthesized under exceptionally mild conditions. Using the cyclization–rearrangement strategy, we recently contributed a gold-catalyzed synthesis of 4-substituted isocoumarine derivatives **8**.[4] The detailed mechanistic investigations revealed an intermolecular transfer of the allyl fragments. Furthermore, a palladium co-catalyst[2y] is not needed in most cases (Scheme 2).

In order to expand this synthetic protocol to other substrates, we envisioned the possibility to form isochromene derivatives by using *ortho*-alkynyl benzylic ethers instead of *ortho*-alkinyl benzoic esters as starting materials. The isochromene motif belongs to the most important pyrane derivatives and can be found in a variety of natural compounds with biological or physiological activity.[5] However, the classical synthetic approaches to isochromenes suffer from harsh reaction conditions and are incompatible with more complex structures.[6,7] The transition-metal-catalyzed cyclizations of *ortho*-alkynyl benzylic alcohols **9** overcome these problems. Yet, another disadvantage persists: After π-philic activation of the multiple bond, the cyclization forms an organometallic intermediate **11** that is rapidly proto-demeta-

[a] Dr. M. Ackermann, J. Bucher, M. Rappold, K. Graf, Dr. F. Rominger, Prof. Dr. A. S. K. Hashmi
Organisch-Chemisches Institut
Universität Heidelberg
Im Neuenheimer Feld 270, 69120 Heidelberg (Germany)

Supporting information for this article is available on the WWW under http://dx.doi.org/10.1002/asia.201300324.

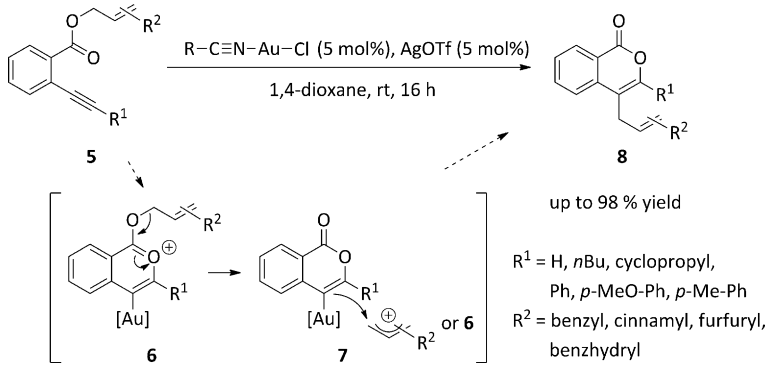

Scheme 2. Synthesis of 4-substituted isocoumarine derivatives **8** using a gold-catalyzed cyclization–rearrangement strategy.

lated by the proton released during the attack of the alcohol (Scheme 3).[8–10] Thus, no substituent other than H can be tethered in the 4-position of **12**.

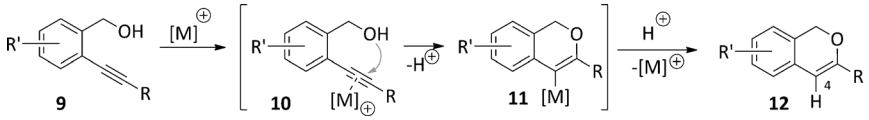

Scheme 3. Transition-metal-catalyzed synthesis of isochromene derivatives **12**.

Herein, we report on our efforts to circumvent this drawback by a cyclization–rearrangement sequence using *ortho*-alkynyl benzylethers (**15**) as starting material. To the best of our knowledge, this strategy has never been used for the synthesis of isochromene derivatives with any transition metal catalyst before.[11] However, the structural skeleton of the starting material was similar to substrates used by Gagosz et al. for the synthesis of highly substituted furans (Scheme 4).[2ac] But, while they used terminal alkynes exclusively without any aromatic backbone (**13**), we anticipated that our substrates **15** may follow a different cyclization mode leading to the six-membered heterocycles **16** instead of isobenzofuran derivatives (Scheme 4).

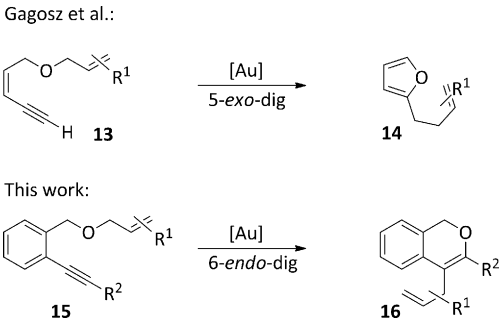

Scheme 4. Comparison of the furan synthesis by Gagosz et al.[2ac] with our current studies.

Results and Discussion

Prior to the catalytic investigations, two test systems were easily prepared in three steps (Scheme 5). First, *ortho*-bromobenzaldehyde **17** was converted into the corresponding alkyne derivatives **18a** and **18b** by Sonogashira coupling, reduction with $NaBH_4$, and subsequent etherification to furnish the desired test substrates **20a** and **20b** in an overall yield of 35% and 39%, respectively.

Our first test reactions with **20a** and **20b** were carried out under the optimized conditions of our isocoumarine synthesis.[4] The substrates were added to a stirred solution of 5 mol% catalyst **K1** and 5 mol% AgOTf in technical grade 1,4-dioxane at room temperature. After 16 hours, full conversion was achieved for both test substrates. However, the isolated yield for phenyl-substituted isochromene **21a** was unsatisfactory (18%), while product **21b** containing the alkyl substituent was isolated in an acceptable yield of 66% (Scheme 6). To our delight, no traces of the simple cyclization product **22**, which could have been formed by a competing protodeauration pathway, were detected.

The ^{1}H NMR spectra clearly proved that the new C–C bond of the rearranged cyclization products had been formed exclusively with inversion of the cinnamyl fragment (Figure 1).

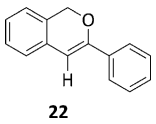

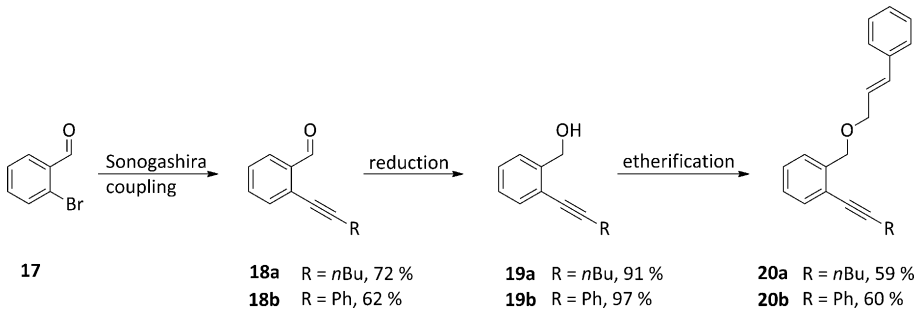

Scheme 5. Synthetic approach to the test systems.

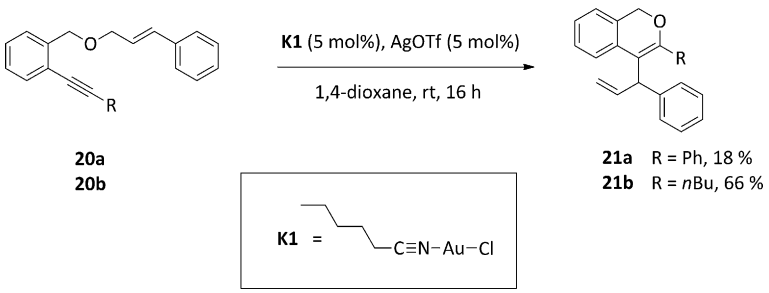

Scheme 6. Gold-catalyzed conversion of substrates **20a** and **20b**.

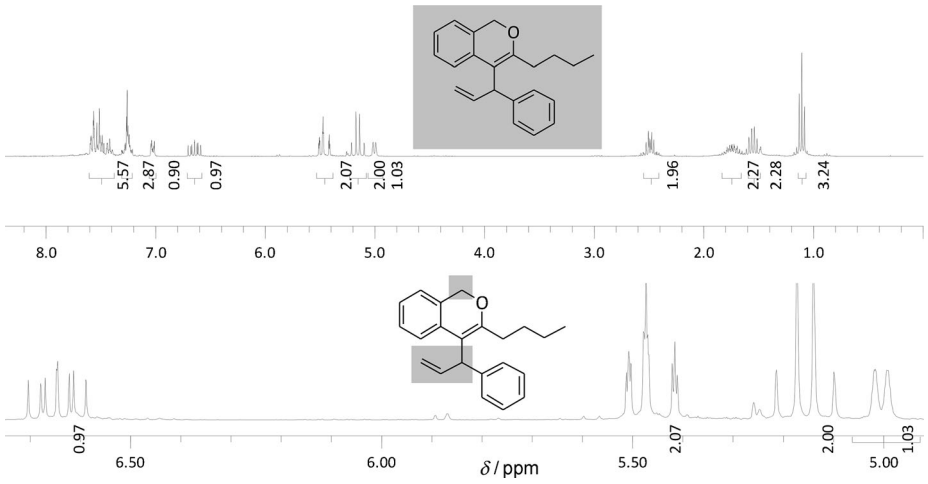

Figure 1. ^{1}H NMR spectrum of **21b** with a branched cinnamyl side chain.

This is noteworthy, as the corresponding ester derivatives always retained the linear structure of the transformed moiety.[4]

Both of these facts gave us first hints about the possible reaction mechanism that seemed to differ from the mechanism of the gold-catalyzed isocoumarine synthesis. Before exploring the scope of this reaction, we first wanted to optimize the reaction conditions with regard to different gold catalysts, counterions, solvents, and temperatures. First, we screened different ligands at the gold center. The test substrate **20a** that has a huge potential for optimization was used. The results are shown in Table 1.

With $AgNTf_2$ as a catalyst-activating additive, 1,4-dioxane as the solvent, and the reaction being carried out at 70 °C, the gold catalyst **K1** with the pentylisonitrile ligand delivered only poor yields of the desired product (entry 1; 36 %). The same is true for the acyclic aminocarbene ligand (entry 2; 20 %), the phosphite ligand (entry 3; 33 %), and the bulky (bisadamantyl)-*n*-butyl-phosphane ligand (entry 4; 31 %). Slightly better results were obtained with the Ph_3PAu catalyst **K5** (entry 5, 54 %). The commercially available IPr gold catalyst **K6** provided product **21a** with 81 % yield, probably due to its higher thermal stability under the indicated conditions (entry 6). The SPhos ligand containing a biaryl-phosphane motif delivered isochromene **21a** in an excellent yield of 98 % (entry 7). Gold(III) chloride turned out to be completely inactive in this reaction (entry 8). In the absence of any gold complex, no conversion of the starting material was observed; neither the silver salt itself nor *p*-TsOH as a Brønsted acid showed catalytic activity (entries 9 and 10). Notably, the expected protodeauration by-product **22** was not detectable in any of the experiments, although technical grade solvent and open-flask conditions were applied.

With **K7** as the best catalyst in hand, we then determined the influence of different counterions on the reaction (Table 2). The control experiment without any activation of the gold catalyst showed no conversion of the starting material (entry 1). AgOAc (entry 2), $Ag(CO_2CF_3)$ (entry 3), AgOTs (entry 4), and the silver salt of binolphosphate (entry 5, 5 mol % each) were not efficient for the activation. AgOTf (entry 6, 65 %), AgONf (entry 7, 67 %), and $AgNTf_2$ (entry 8, 78 %) gave good results after 16 hours. Even higher yields were achieved when $AgPF_6$ (entry 9, 85 %) or $AgSbF_6$ (entry 10, 100 %) were used for the activation of the gold catalyst, most probably due to their spherical symmetry shape, which results in their lowest coordination tendency.

Finally, different solvents were investigated (Table 3). Optimized conditions from the earlier screenings were applied (5 mol % of [SPhosAuCl] and 5 mol % of $AgNTf_2$, Table 1, entry 7). In order to enable milder conditions, all of the reactions were performed at room temperature.

1,4-Dioxane (entry 1, 71 %) delivered only moderate yields, but the other tested solvents significantly improved the yields, no matter if protic (MeOH, entry 2, 88 %), polar nonprotic (acetonitrile, entry 3, 85 %), or non-polar solvents were applied (benzene, entry 4, 90 %). Excellent results were obtained in DMF (entry 5, 97 %), diethyl ether (entry 6, 98 %), or CH_2Cl_2 (entry 7, 100 %). In all of these solvents, no traces of by-products were detected.

Under these optimized conditions, we next explored the scope and limitations of this domino reaction with a small library of differently substituted (*ortho*-alkynyl benzylic) ethers. Two possible approaches to the starting materials were investigated. Firstly, a three-step protocol using *ortho*-bromo benzaldehyde **17** as a starting material and utilizing Sonogashira coupling, reduction with $NaBH_4$, and subsequent etherification of the benzylic alcohol was examined

Table 1. Optimization with **20a** and different gold catalysts.

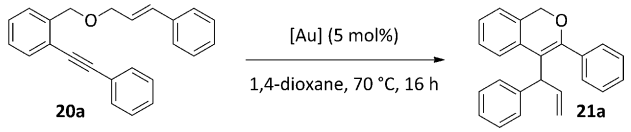

Entry	Catalyst		$AgNTf_2$	Yield of **21a** [%][a,b]
1	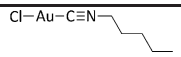	**K1**	5 mol%	36
2	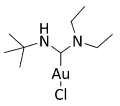	**K2**	5 mol%	20
3	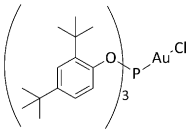	**K3**	5 mol%	33
4	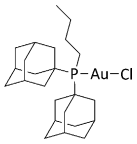	**K4**	5 mol%	31
5	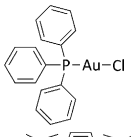	**K5**	5 mol%	54
6	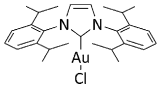	**K6**	5 mol%	81
7	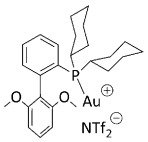	**K7**	–	98
8	$AuCl_3$	**K8**	–	22
9	–	–	5 mol%	0
10	*p*-TsOH	–	–	0

[a] Yields were determined by GC/MS in the presence of *n*-dodecane as an internal standard. [b] The cinnamylic fragment was incorporated in a branched fashion in all cases.

Table 2. Optimization with **20a** and different counterions.

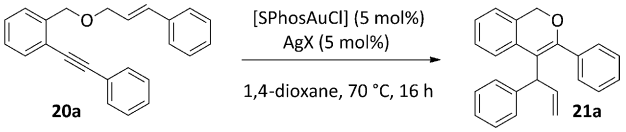

Entry	Silver salt AgX	Yield of **21a** [%][a,b]
1	–	0
2	^-OAc	0
3	$CF_3CO_2^-$	0
4	^-OTs	2
5	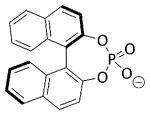	1
6	^-OTf	65
7	^-ONf	67
8	NTf_2^-	78
9	PF_6^-	85
10	SbF_6^-	100

[a] Yields were determined by GC/MS in presence of *n*-dodecane as an internal standard. [b] The cinnamylic fragment was incorporated in a branched fashion in all cases.

Table 3. Optimization with **20a** and different solvents.

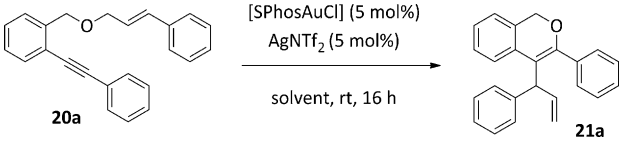

Entry	Solvent	Yield of **21a** [%][a,b]
1	1,4-Dioxane	71
7	MeOH	88
5	CH_3CN	85
6	Benzene	90
4	DMF	97
2	Et_2O	98
3	CH_2Cl_2	100

[a] Yields were determined by GC/MS in presence of *n*-dodecane as an internal standard. [b] The cinnamylic fragment was incorporated in a branched fashion in all cases.

(Scheme 7). Secondly, a two-step protocol was applied starting from *ortho*-iodobenzylic alcohol **23**. Etherification, followed by a Sonogashira coupling (Scheme 7) delivered the desired starting materials. The preferred route for varying the ether substituent was the one according to Scheme 4, while the alternative path according to Scheme 6 was preferably chosen when the alkyne motif needed to be diversified.

Based on the easy accessibility of the starting materials, an array of substrates was prepared within a short time in overall yields ranging from 27 to 80%. The results of the successive cyclization–rearrangement sequence induced by our optimized catalytic conditions are summarized in Table 4. Our special attention was focused on the cyclization manner (5-*exo*-dig vs. 6-*endo*-dig) as well as on the binding properties of the rearranged fragments that could be either linear (without allylic inversion) or branched (with allylic inversion).

The substrate **20c** bearing a simple allylic group was isomerized successfully to the expected allylic isochromene derivative **21c** with good yield (entry 1, 66%). Excellent yields were obtained with crotyl- (entry 2, 99%) and prenyl-ethers (entry 3, 99%). The latter one caused the formation of a quaternary carbon center after the completion of the rearrangement. Even with the cyclic allylic system in compound **20f**, the

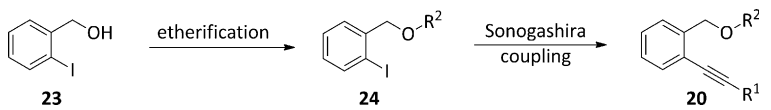

Scheme 7. Alternative access to a variety of substrates **20**.

Table 4. Scope and limitations of the gold-catalyzed isochromene synthesis with allyl transfer.

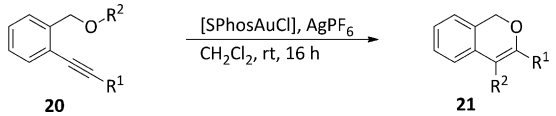

20 21

Entry	Starting material		Catalyst	Producct		Yield [%][a]
1[b,c,f]	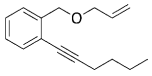	**20c**	5 mol %[d]	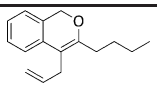	**21c**	66
2[e,f]	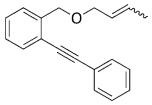	**20d**	2 mol %	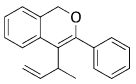	**21d**	99
3[e,f]	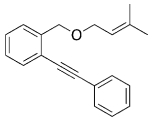	**20e**	2 mol %	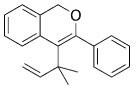	**21e**	99
4	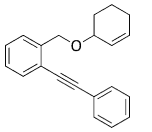	**20f**	2 mol %	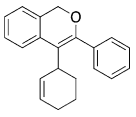	**21f**	99
5	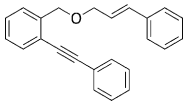	**20a**	5 mol %	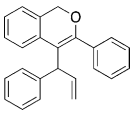	**21a**	99
6	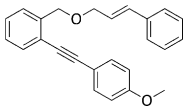	**20g**	5 mol %	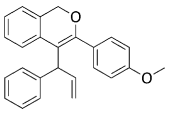	**21g**	99
7	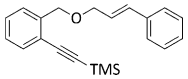	**20h**	2 mol %	decomposition	–	–
8	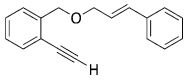	**20i**	5 mol %	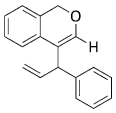	**21i**	50
9	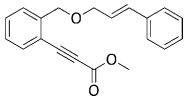	**20j**	5 mol %	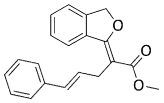	**21j**	14
10[g]	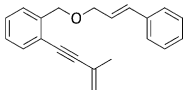	**20k**	5 mol %	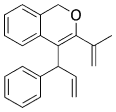	**21k**	67
11[e]	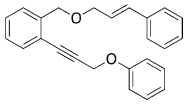	**20l**	2 mol %	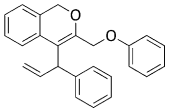	**21l**	96
12	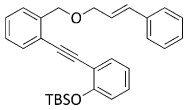	**20m**	2 mol %	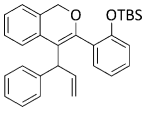	**21m**	68
13	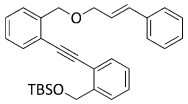	**20n**	2 mol %	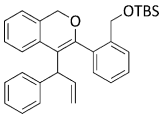	**21n**	77
14	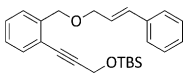	**20o**	5 mol %	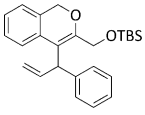	**21o**	<5 (92)[h]

result of the cyclization–rearrangement sequence was stunning (entry 4, 99%). We further tested a wide range of differently substituted cinnamylic ether substrates with varying electronic and steric properties at the alkyne terminus. While the compounds with a phenyl substituent such as **20a** (entry 5, 99%) or with the more electron-rich *para*-methoxyphenyl substituent (**20g**, entry 6, 99%) afforded the corresponding isochromenes with excellent yields, compound **20h** with a trimethylsilyl (TMS) substituent decomposed under these conditions (entry 7). After all, compound **20i** with a terminal acetylene substituent gave the isochromene **21i** in moderate yields (entry 8, 50%). Despite the fact that the activation of terminal aryl acetylene moieties by gold catalysts does not normally favor an endocyclic ring closure, the 6-membered heterocyclic substructure was confirmed unambiguously by ^{1}H NMR coupling constant analysis (Figure 2) and 2D-NMR experiments, namely HSQC(me) and HBMC. Only when the polarization of the triple bond was inverted by a CO_2Me substituent, was the 6-*endo*-dig cyclization mode suppressed and a complex reaction mixture observed (entry 9). The only product isolated, with a low yield of 14%, was **21j**, wherein the ring closure had followed a 5-*exo*-*dig* mode and the rearranged cinnamylic fragment was rebounded in a linear fashion without previous allylic inversion. However, a further olefinic functionality in conjugation with the alkyne was tolerated and delivered the corresponding isochromene **21k** in a good yield (entry 10; 67%). Compound **20l** with an oxygen atom in the tether reacted selectively to the isochromene

Table 4. (Continued)

Entry	Starting material		Catalyst	Producct		Yield [%][a]
15	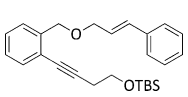	**20p**	5 mol%	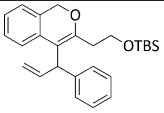	**21p**	30 (99)[h]
16	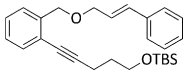	**20q**	5 mol%	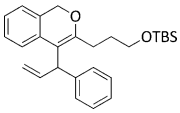	**21q**	57 (99)[h]
17	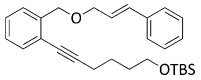	**20r**	5 mol%	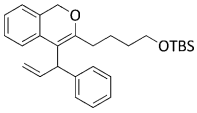	**21r**	28
18	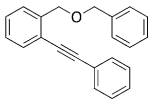	**20s**	5 mol%	–	–	0
19[b,c]	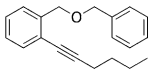	**20t**	5 mol%[c]	–	–	0
20	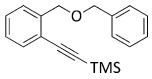	**20u**	2 mol%	–	–	0

[a] Isolated yields. [b] The gold catalyst was activated with AgOTf; 1,4-dioxane was used as the solvent. [c] Alternative reaction conditions did not improve the yield. [d] **K1** was used as the catalyst. [e] 1,2-Dichloroethane was used as the solvent. [f] The reaction was carried out at 70 °C. [g] **K6** was used as the catalyst and activation was done with $AgNTf_2$. [h] The yields in parentheses were determined by integration of ^{1}H NMR signals of the raw product using hexamethylbenzene as an internal standard.

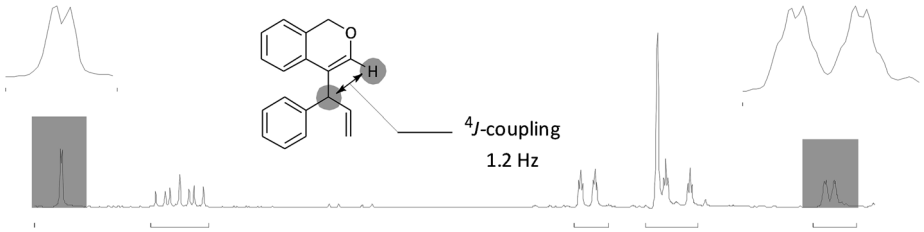

Figure 2. ^{1}H NMR of compound **21i**. The specific ^4J-coupling confirms its structure.

derivative **21l** with 96% yield (entry 11). Inspired by this result, we further went on testing other substrates with ether functionalities. The TBS-protected phenyl ether substituent (entry 12, 68%) was as well tolerated as the TBS-protected benzylether substituent (entry 13, 77%). Moreover, a series of alkyl substituents with terminal TBS ether functionalities were tested. Different chain lengths were present in these substrates and once more the isochromenes were formed exclusively (entries 14–17). Since the isolated yields were poor to moderate, we followed the reaction by continuous NMR studies. The excellent yields determined by NMR spectroscopy with hexamethyl benzene as an internal standard (entries 14–16, 92–99%) indicated that the aforementioned poor results may have originated from problems during the work-up and purification procedures. All of these compounds accomplished the ring closure selectively over the cinnamylic ether oxygen—a competing nucleophilic attack of the silylether oxygen on the triple bond did not occur. After the extensive study on allylic and cinnamylic derivatives, we turned to benzylic starting materials (entries 18–20). Despite the fact that successful similar rearrangements of benzylic ethers have been described with other substrates before,[2p,t,v,w,z,ae,af,4] no conversion of any of the tested benzylic ethers was observed in our reaction, even at elevated temperatures. The starting material was recovered in each individual case. A plausible reason for that behavior will be presented below in connection with a discussion of the reaction mechanism.

Even though the connectivity, the scope, and the limitations gave us valuable hints concerning a plausible reaction mechanism, we additionally carried out several experiments to verify our assumptions. The spectroscopic data of the purified products from Table 4 clearly proved the branched C–C bond coupling manner, which was obviously caused by an allylic inversion rather than by an entire dissociative fragmentation. This result is exemplified by the ^{1}H NMR spectrum of compound **21b** in Figure 1. The cyclization mode that we assumed before to be 6-*endo*-dig rather than 5-*endo*-dig was also confirmed representatively by NMR spectroscopy of compound **21i** (Figure 2) and X-ray crystal structure analysis of compound **21k** (Figure 3).[12] The branched fashion of the cinnamylic fragment is obvious as well.

Another striking observation was the lack of a C^4-unsubstituted by-product by protodeauration even if significant traces of water were present or *p*-TsOH (5 mol%) was added to the reaction mixture. This is all the more surprising as our related isocoumarine synthesis always afforded by-products from a competing protodeauration.[4] On the other hand, no effect on the reaction rate was observed by exclusion of moisture using Schlenk-flask techniques, addition of 4 Å molecular sieves, and dry solvents. This means that protons unlikely take part in the reaction mechanism. Most likely, the gold-mediated cyclization leads to an organogold oxonium species **B** that undergoes an intramolecular [3,3]-sigmatropic rearrangement to **C** instead of heterolytic cleavage with formation of an ion pair and subsequent migration of the carbocationic fragment. The catalytic cycle closes

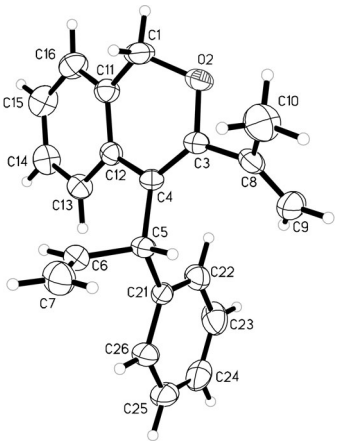

Figure 3. X-ray crystal structure of compound **21k** confirming the 6-*endo-dig* cyclization mode.Thermal ellipsoids are drawn at the 50% probability level.

with the heterolytic cleavage of the gold–carbon bond, thereby regenerating the active gold catalyst and forming the product **21** (Scheme 8).

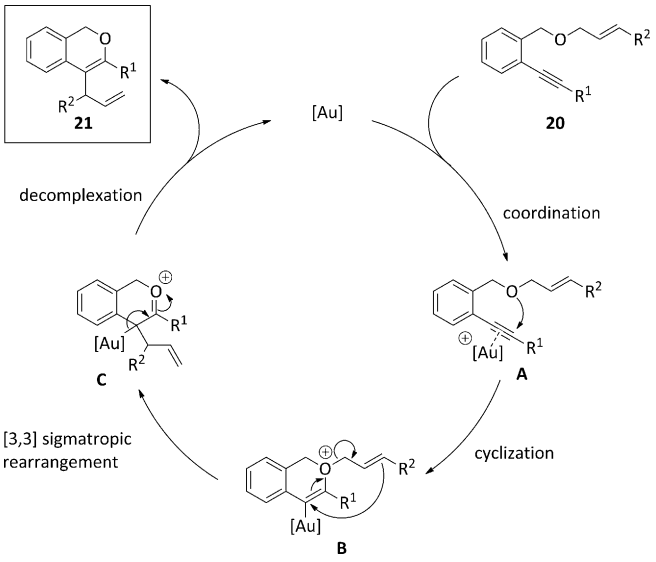

Scheme 8. Mechanism proposed for the gold-catalyzed isochromene synthesis.

The mechanistic proposal is in accordance with the previous work of Gagosz et al. who also observed a [3,3]-sigmatropic key step for the rearrangement of the allyl moieties after a gold-catalyzed cyclization step.[2ac]

To provide further evidence of the mechanism, we further performed a crossover experiment which clearly ruled out an intermolecular process (Scheme 9). Under the denoted conditions, compounds **20c** and **20v** at a ratio of 1:1 were converted straight into the products **21c** and **21v** without any traces of crossover products **21w** and **21x** as confirmed by gas chromatography–mass spectrometry (GC–MS).

Furthermore, the proposed mechanism is in accordance with the observation that benzylic substituents did not lead to the desired isochromene derivatives at all (Table 4, entries 17–19). For this reaction path, the ability to undergo a sigmatropic rearrangement rather than the ability to stabilize a positive charge seems to be crucial. In the case of benzylic ether substituents, this kind of sigmatropic rearrangement would be accompanied by a temporary interruption of the aromatic system (in an intermediate **27**) and thus would be energetically unfavored (Scheme 10; the situation reminds of the *ortho*-Claisen rearrangement, but seemingly the thermal window of stability of the gold catalyst is not compatible with the temperatures needed for the subsequent [3,3]sigmatropic rearrangement).

Conclusions

This mild and efficient approach to isochromene derivatives by a cyclization–rearrangement strategy using homogeneous gold catalysis allows the synthesis of specific substitution patterns. Under optimized conditions, a variety of substrates with different steric and electronic properties could be converted with excellent yields and selectivity, even if air or moisture was not excluded. Mechanistic investigations based on spectroscopic data, control experiments, crossover experiments, and the reaction scope clearly indicated an intramolecular mechanism composed of a gold-catalyzed cyclization step and a [3,3]-sigmatropic rearrangement with formal inversion of the allylic moiety. To the best of our knowledge, this is the first example where such a domino reaction is used for the formation of isochromene derivatives and where the mechanism is clearly different from the intermolecular allyl transfer in the corresponding allyl *ortho*-alkynyl benzoates.

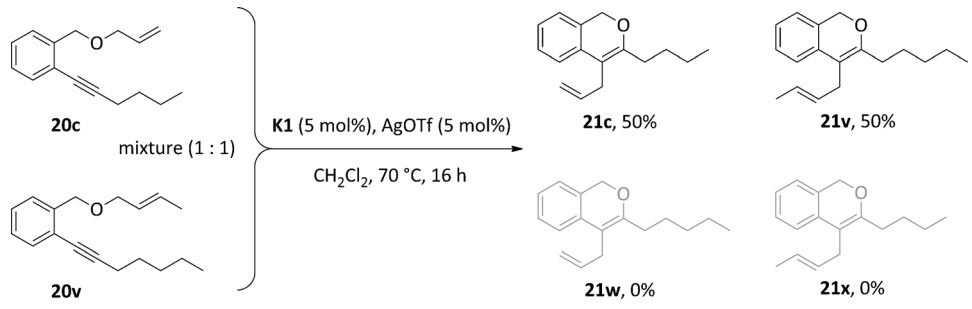

Scheme 9. Crossover experiment confirming the intramolecular nature of the allyl transfer.

Experimental Section

Procedures for the synthesis of compounds and characterization data of compounds are given in the Supporting Information.

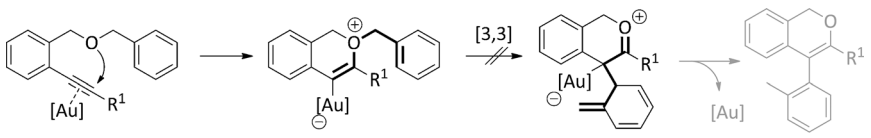

Scheme 10. A rearrangement of the benzylic substituents with temporary interruption of the aromatic system does not occur.

Acknowledgements

This work was supported by the Deutsche Forschungsgemeinschaft (SFB 623); we thank Umicore AG&Co. KG for the generous donation of noble metal salts.

[1] T. Tsuda, Y. Ohashi, N. Nagahama, R. Sumiya, T. Saegusa, *J. Org. Chem.* **1988**, *53*, 2650–2653.

[2] a) T. Mandai, K. Ohta, N. Baba, M. Kawada, J. Tsuji, *Synlett* **1992**, 671–672; b) S. Cacchi, G. Fabrizi, P. Pace, *J. Org. Chem.* **1998**, *63*, 1001–1011; c) S. Cacchi, G. Fabrizi, L. Moro, *Synlett* **1998**, 741–746; d) N. Monteiro, G. Balme, *Synlett* **1998**, 746–747; e) S. Cacchi, G. Fabrizi, L. Moro, *Tetrahedron Lett.* **1998**, *39*, 5101–5104; f) S. Kamijo, Y. Yamamoto, *J. Am. Chem. Soc.* **2002**, *124*, 11940–11945; g) A. Fürstner, H. Szillat, F. Stelzer, *J. Am. Chem. Soc.* **2000**, *122*, 6785–6786; h) A. Fürstner, F. Stelzer, H. Szillat, *J. Am. Chem. Soc.* **2001**, *123*, 11863–11869; i) T. Shimada, I. Nakamura, Y. Yamamoto, *J. Am. Chem. Soc.* **2004**, *126*, 10546–10547; j) I. Nakamura, Y. Mizushima, Y. Yamamoto, *J. Am. Chem. Soc.* **2005**, *127*, 15022–15024; k) A. Fürstner, P. W. Davies, *J. Am. Chem. Soc.* **2005**, *127*, 15024–15025; l) A. Fürstner, E. K. Heilmann, P. W. Davies, *Angew. Chem.* **2007**, *119*, 4844–4847; *Angew. Chem. Int. Ed.* **2007**, *46*, 4760–4763; m) I. Nakamura, Y. Mizushima, U. Yamagishi, Y. Yamamoto, *Tetrahedron* **2007**, *63*, 8670–8676; n) K. Cariou, B. Ronan, S. Mignani, L. Fensterbank, M. Malacria, *Angew. Chem.* **2007**, *119*, 1913–1916; *Angew. Chem. Int. Ed.* **2007**, *46*, 1881–1884; o) I. Nakamura, C. S. Chan, T. Araki, M. Terada, Y. Yamamoto, *Org. Lett.* **2008**, *10*, 309–312; p) I. Nakamura, T. Sato, Y. Yamamoto, *Angew. Chem.* **2006**, *118*, 4585–4587; *Angew. Chem. Int. Ed.* **2006**, *45*, 4473–4475; q) I. Nakamura, U. Yamagishi, D. Song, S. Konta, Y. Yamamoto, *Angew. Chem.* **2007**, *119*, 2334–2337; *Angew. Chem. Int. Ed.* **2007**, *46*, 2284–2287; r) I. Nakamura, T. Sato, M. Terada, Y. Yamamoto, *Org. Lett.* **2007**, *9*, 4081–4083; s) F. M. Istrate, F. Gagosz, *Org. Lett.* **2007**, *9*, 3181–3184; t) I. Nakamura, T. Sato, M. Terada, Y. Yamamoto, *Org. Lett.* **2008**, *10*, 2649–2651; u) G. Li, X. Huang, L. Zhang, *Angew. Chem.* **2008**, *120*, 352–355; *Angew. Chem. Int. Ed.* **2008**, *47*, 346–349; v) T. Sato, I. Nakamura, M. Terada, *Eur. J. Org. Chem.* **2009**, 5509–5512; w) M. Uemura, I. G. D. Watson, M. Katsukawa, F. D. Toste, *J. Am. Chem. Soc.* **2009**, *131*, 3464–3465; x) T. S. A. Heugebaert, C. V. Stevens, *Org. Lett.* **2009**, *11*, 5018–5021; y) Y. Shi, K. E. Roth, S. D. Ramgren, S. Blum, *J. Am. Chem. Soc.* **2009**, *131*, 18022–18023; z) H. Aikawa, S. Tago, K. Umetsu, N. Haginiwa, N. Asao, *Tetrahedron* **2009**, *65*, 1774–1784; aa) M. Ueda, A. Sato, T. Miyoshi, T. Naito, O. Miyata, *Org. Lett.* **2010**, *12*, 2594–2597; ab) I. Nakamura, M. Okamoto, T. Sato, M. Terada, *Heterocycles* **2010**, *82*, 689–697; ac) F. M. Istrate, F. Gagosz, *Beilstein J. Org. Chem.* **2011**, *7*, 878–885; ad) J. Y. Cheong, D. Im, M. Lee, W. Lim, Y. H. Rhee, *J. Org. Chem.* **2011**, *76*, 324–327; ae) J. Renault, Z. Qian, P. Uriac, N. Gouault, *Tetrahedron Lett.* **2011**, *52*, 2476–2479; af) K. Komeyama, K. Takahashi, K. Takaki, *Org. Lett.* **2008**, *10*, 5119–5122; ag) P.-Y. Chiang, Y.-C. Lin, Y. Wang, Y.-H. Liu, *Organometallics* **2010**, *29*, 5776–5782.

[3] For selected reviews, see: a) A. S. K. Hashmi, *Gold Bull.* **2004**, *37*, 51–65; b) A. S. K. Hashmi, G. J. Hutchings, *Angew. Chem.* **2006**, *118*, 8064–8105; *Angew. Chem. Int. Ed.* **2006**, *45*, 7896–7936; c) R. A. Widenhoefer, X. Han, *Eur. J. Org. Chem.* **2006**, 4555–4563; d) A. S. K. Hashmi, *Chem. Rev.* **2007**, *107*, 3180–3211; e) A. Fürstner, P. W. Davies, *Angew. Chem.* **2007**, *119*, 3478–3519; *Angew. Chem. Int. Ed.* **2007**, *46*, 3410–3449; f) E. Jiménez-Núñez, A. M. Echavarren, *Chem. Rev.* **2008**, *108*, 3326–3350; g) Z. Li, C. Brouwer, C. He, *Chem. Rev.* **2008**, *108*, 3239–3265; h) A. Arcadi, *Chem. Rev.* **2008**, *108*, 3266–3325; i) D. J. Gorin, B. D. Sherry, F. D. Toste, *Chem. Rev.* **2008**, *108*, 3351–3378; j) N. T. Patil, Y. Yamamoto, *Chem. Rev.* **2008**, *108*, 3395–3442; k) A. S. K. Hashmi, M. Bührle, *Aldrichimica Acta* **2010**, *43*, 27–33; l) A. Corma, A. Leyva-Pérez, M. J. Sabater, *Chem. Rev.* **2011**, *111*, 1657–1712.

[4] A. S. K. Hashmi, C. Lothschütz, R. Döpp, M. Ackermann, J. De Buck, M. Rudolph, C. Scholz, F. Rominger, *Adv. Synth. Catal.* **2012**, *354*, 133–147.

[5] For examples, see: a) M. Shamma, D.-Y. Hwang, *Tetrahedron* **1974**, *30*, 2279–2282; b) P. L. Majumder, E. Sabzabadi, *Phytochemistry* **1988**, *27*, 1899–1901; c) P. L. Majumder, S. Sen, S. Benerjee, *Tetrahedron* **1999**, *55*, 6691–6702; d) J. Gripenberg, L. Hiltunen, T. Pakkanen, T. Pakkanen, *Acta Chem. Scand.* **1979**, *33b*, 6–10; e) J. Gripenberg, L. Hiltunen, L. Niinistö, T. Pakkanen, T. Pakkanen, *Acta Chem. Scand.* **1979**, *33b*, 1–5; f) C. P. Ndi, S. J. Semple, H. J. Griesser, S. M. Pyke, M. D. Barton, *J. Nat. Prod.* **2007**, *70*, 1439–1443.

[6] A. S. Bailey, C. R. Worthing, *J. Chem. Soc.* **1956**, 4535–4543.

[7] J. N. Chatterjea, *Chem. Ber.* **1958**, *91*, 2636–2638.

[8] B. Gabriele, G. Salerno, A. Fazio, R. Pittelli, *Tetrahedron* **2003**, *59*, 6251–6259.

[9] X. Li, A. R. Chianese, T. Vogel, R. H. Crabtree, *Org. Lett.* **2005**, *7*, 5437–5440.

[10] A. S. K. Hashmi, S. Schäfer, M. Wölfle, C. D. Gil, P. Fischer, A. Laguna, M. C. Blanco, M. C. Gimeno, *Angew. Chem.* **2007**, *119*, 6297–6300; *Angew. Chem. Int. Ed.* **2007**, *46*, 6184–6187.

[11] For an iodine initiated cyclization, see: a) R. Mancuso, S. Mehta, B. Gabriele, G. Salerno, W. S. Jenks, R. C. Larock, *J. Org. Chem.* **2010**, *75*, 897–901; b) L. Su, C.-Y. Lei, W.-Y. Fan, L.-X. Liu, *Synth. Commun.* **2011**, *41*, 1200–1207.

[12] CCDC 930859 (**21k**) contains the supplementary crystallographic data for this paper. These data can be obtained free of charge from The Cambridge Crystallographic Data Centre via www.ccdc.cam.ac.uk/data_request/cif.

Received: March 12, 2013
Published online: ■■ ■■, 0000